Applied Magnetic Resonance (2021) 52:99–115
https://doi.org/10.1007/s00723-020-01273-3

Applied
Magnetic Resonance

ORIGINAL PAPER

The Use of Single-Sided NMR to Study Moisture Behaviour in an Activated Carbon Fibre/Phenolic Composite

Sue Alston[1] · Cris Arnold[1] · Martin Swan[2] · Corinne Stone[2]

Received: 2 June 2020 / Revised: 22 August 2020 / Accepted: 21 September 2020 /
Published online: 6 October 2020

Abstract

Nuclear Magnetic Resonance (NMR) has been shown to be a useful technique to study the form and content of water in polymer composites. Composites using activated carbon fibres with phenolic resin have complex water absorption behaviour which would benefit from such investigation; however, the presence of the conductive fibres can make NMR problematic. In this study, single-sided NMR has been successfully used on such material by developing a method for sample-to-sample compensation for the effect of conductivity. Transverse relaxation curves showed water to be primarily in two states in the resin, corresponding to "bound" and "mobile" molecules. In addition, two much less bound states were identified in the composite, associated firstly with water adsorbed on to the fibre surface and secondly with clusters of water molecules moving more freely within the fibre pores.

List of Symbols

A	Amplitude of fitted echo amplitude curve (microvolts)
A_i	Amplitude of component i of fitted echo amplitude curve, with time constant t_i, $i=1$ (shortest) to 4 (longest) (microvolts)
$\overset{\frown}{Curve\ area}$	Area under CPMG curve calculated from fitted echo amplitude curve
$\overline{Curve\ area}$	Estimate of *Curve area* for a single condition, from linear fitting against reflected signal minimum
k	Ratio of α/β averaged over all conditions.

✉ Sue Alston
sue.alston@cantab.net

Cris Arnold
j.c.arnold@swansea.ac.uk

Martin Swan
mswan@mail.dstl.gov.uk

Corinne Stone
cstone@mail.dstl.gov.uk

[1] College of Engineering, Swansea University, Fabian Way, Swansea SA1 8EN, UK

[2] Defence Science and Technology Laboratory, Porton Down, Salisbury SP4 0JQ, UK

t	Echo time (ms)
t_i	Time constant of component i of fitted echo amplitude curve, $i = 1$ (shortest) to 4 (longest) (ms)
α	Slope obtained from fitting of *Curve area* against reflected signal minimum for a single condition
$\hat{\alpha}$	Estimate of α from linear fitting of α vs β
β	Intercept obtained from fitting of *Curve area* against reflected signal minimum for a single condition
μ	Scaling factor to be applied to measured amplitudes
φ	Reflected signal minimum

1 Introduction

1.1 Use of Carbon/Phenolic Composites

Carbon fibre/phenolic composites are used in applications requiring the mechanical properties of carbon fibre combined with the fire resistant or high temperature behaviour of phenolic resin. This includes, for example, thermal protection systems for space or rocket applications. The material may experience extreme temperatures and rapid temperature changes, leading to mechanical and thermo-mechanical damage [1].

Polymerisation of phenolic resins is a condensation reaction producing water, a proportion of which, typically a few percent by weight, remains in the material at the end of the cure process. Between manufacture and use, components may be stored, and the water content may change.

The carbon fibres used in such composites may be fully graphitised, in which case they are assumed to absorb no water, although there may be some interface/interphase effects. However, of particular interest for this study were activated carbon fibres which retain some porosity. The water content of composites using such fibres has been shown to have a non-linear dependency on relative humidity [2], and this was attributed to the presence of at least two water-absorbing phases. Investigation of the mechanism for water ingress to and egress from these fibres by Do and Do [3] proposed that water was initially adsorbed on to the fibre surface, then migrated into the pores when sufficiently large clusters of water molecules had built up.

The importance of the water content, and the relative complexity of its behaviour in this composite material, makes it an ideal candidate material for in-depth study, and the ability to assess in detail the form in which water is held would be beneficial. This study attempted to gain a better understanding of this using a single-sided Nuclear Magnetic Resonance (NMR) technique.

1.2 NMR Mouse

The "NMR MOUSE" (MObile Universal Surface Explorer) produced by Magritek is a portable, open NMR sensor with a permanent magnet geometry

that generates a flat sensitive volume parallel to the scanner surface [4]. Unlike conventional NMR, it operates at a single frequency, which for this study corresponded to ^{1}H protons. A schematic of the instrument as used for a small sample is shown in Fig. 1.

The sample is placed above a permanent magnet and radio frequency (RF) probe, which can be moved vertically. The probe position determines the location of a measured "slice" within the sample. The RF probe manipulates the magnetic moment of the hydrogen nuclei and produces a "spin-echo" signal by a suitable sequence of pulses, which provides information on the rate of decay of the induced moment. The decay of signal due to transverse (T_2) relaxation depends on the magnetic field effect of neighbouring nuclei and is fastest where neighbouring nuclei have most effect. So, for example the T_2 time constant is low in the case of covalent bonding and high in the case of free water. This distinction made the use of T_2 relaxation a suitable choice for investigation of the form in which water was held in the composite.

Single-sided NMR was originally developed to investigate fluids within pores in rocks or building materials, where it was necessary to take NMR to the sample rather than the sample to NMR. The overall development of the technology, its operation and applications have been reviewed and detailed by Blümich et al. [5, 6] and Casanova et al. [7]. In an example related to polymers and composites, Guthausen et al. [8] used the NMR Mouse to characterise elastomers, using T_2 relaxation tuned to hydrogen nuclei. Typical relaxation times were around 5 ms and were found to vary with cross-link density and ageing. They compared results with those from conventional NMR and found that the signal-to-noise ratio was lower, but that trends with material properties were comparable.

Conventional NMR has previously been used to look at water content in polymers [9]. The use of single-sided NMR, to investigate the absorption of water by PVC, was reported by Kolz [10]. Measurements were taken at 200-micron spacings through a 3 mm sample, and the amplitude of the echo sample converted to an equivalent percentage water content at each point. The readings were repeated periodically, and the resulting through-thickness profiles showed the progress of water absorption.

A previous study using conventional NMR along with gravimetric data [11] identified water in two forms in an epoxy resin. These corresponded to the "mobile" and "bound" water of Langmuir-type diffusion described by Carter and

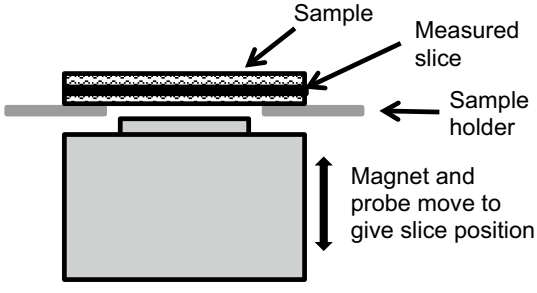

Fig. 1 Schematic of NMR Mouse sample and probe position

Kibler [12], and resulted in a two-stage absorption curve where initial Fickian behaviour was followed by a slow long-term water uptake.

1.3 Conductive Material

The applications described above were for non-conductive material where there is no interference between the RF field and the sample. If a sample is electrically conductive then the varying field can produce eddy currents which weaken the signal and increase the resonant frequency. This can significantly reduce the signal-to-noise ratio. As carbon fibre composites can have some conductivity along the fibres, this can cause problems, but will depend on the fibre lay-up. The lay-up may also mean that the conductivity varies with direction, as reported by Lind et al. [13]. They found that, for cross-ply carbon fibre/epoxy laminates, the effective conductivity of a panel face, where conduction could take place along the fibres, was found to be 200 times greater than that of an edge, where conduction took place from fibre-to-fibre across plies. They reported that this difference affected NMR imaging, so that images could be taken up to ~ 1 cm in from the edge, but less than 2 mm in from the surface.

A comparison of moisture uptake in epoxy composite reinforced with different fibre types found that, although signals could be obtained for samples with carbon fibre, these were poor compared to those for aramid fibre [14]. NMR images became less clear, signal amplitudes were lower, and the presence of water was only obvious after greater conditioning. Whilst this was attributed to the lower water absorption of carbon fibres compared to aramid fibres, it would also result from the effect of conductivity and the corresponding reduction in signal.

The use of relaxation times to study carbon fibre/epoxy composite samples has been assessed, specifically in relation to thermal damage [15]. Whilst it was possible to identify the effects of thermal treatment using conventional NMR in a homogeneous magnetic field, the signal-to-noise ratios from an NMR MOUSE were too small to distinguish any effect, even using a specially designed probe. Any damage to the sample, through fibres breaking or losing electrical contact, changed the eddy currents and hence the signal.

1.4 Aims

This work was part of an overall project studying a specific carbon fibre/phenolic composite. The material was therefore defined, and the aim was to explore the use of NMR Mouse to investigate water absorption in this case. This would potentially require methods to handle conductivity issues with the carbon fibres. If possible, it was also hoped to obtain through-thickness water concentration profiles to give additional information on diffusion behaviour.

Table 1 Conditioning temperatures and humidities

Temperature	Relative humidity (RH)				
50 °C	Dry		45%		85%
70 °C	Dry	25%	45%	65%	85%

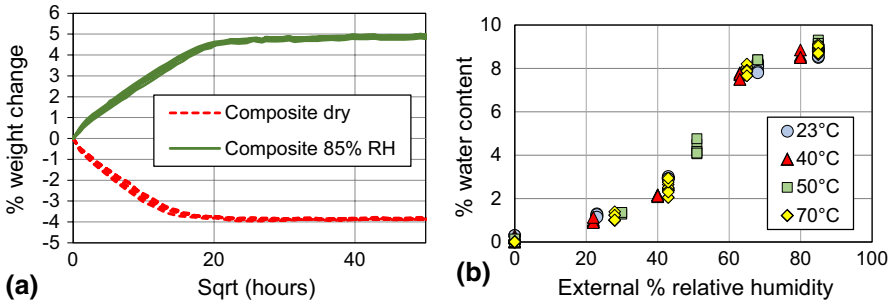

Fig. 2 Conditioning of composite samples. **a** Weight change curves at 70 °C/dry and 70 °C/85% RH. **b** Steady state water content variation with external relative humidity

2 Materials

The composite material under study used a commercially available resole phenolic resin, either alone or reinforced with a woven carbon fabric using activated carbon fibres which retain some porosity. Composite panels were hot pressed and/or clave-cured using a commercial manufacturing process. Samples of resin alone and of the composite were used, between 1 and 2 mm in thickness and either discs of approximately 25 mm in diameter or 25 mm squares.

3 Experimental

3.1 Conditioning

Samples were conditioned to saturation or total drying at a range of temperatures and relative humidities (RH) as shown in Table 1. The loss or gain of water was monitored by gravimetric tests, with weight measurements taken at increasing time intervals, each approximating to one on a $\sqrt{(\text{hours})}$ scale. Examples of the weight change for samples conditioned at 70 °C, and dry or 85% RH, are plotted as a function of $\sqrt{(\text{hours})}$ in Fig. 2a. The steady state water content relative to the totally dried state is shown in Fig. 2b, for various humidities and temperatures. The sigmoidal shape has previously been attributed to the porosity of the fibres, which adsorbed/absorbed water mostly between 30 and 70% RH [2]. NMR Mouse tests were initially carried out on samples in the as-manufactured state, then repeated on conditioned samples.

3.2 NMR Mouse Settings

A Carr–Purcell–Meiboom–Gill (CPMG) sequence was used to obtain the T_2 relaxation signal, giving a measurement of echo amplitude as a function of time. Initial tests for the composite were carried out on samples where the plane of the sample was parallel to the lay-up plane of the fabric. However, no signal could be obtained from these, and this was ascribed to the conductivity of the fibres and hence generation of eddy currents. In an attempt to reduce this effect by restricting the continuity of fibre contacts, samples 1-mm thick were machined at an angle of 20° to the lay-up plane.

It proved possible to obtain a useable signal from these samples, although considerable tuning was still required as the signal-to-noise ratio was low, and a large number of repeat scans were averaged to give a reliable trace. The parameters required are explained in Table 2, which also lists the values used after tuning.

In order to improve the signal, a low acquisition time was needed. This increased the acquisition bandwidth, so that a signal was detected over a greater frequency range, corresponding to a greater slice thickness. The 4 μsec acquisition time used gave a slice thickness of around 200 microns.

Two factors in these settings affected the ability to measure water concentration profiles through the sample thickness. One was the slice thickness, which at 200 microns gave only five slices within the 1 mm thick sample. The second was the large number of repeated scans required (1000), which meant that each reading took around 20 min. Testing was carried out in a temperature-controlled lab, but the test itself caused some heating of the sample, up to around 45 °C. This would have slightly increased the rate of moisture exchange with the ambient lab atmosphere, so had the potential to change the surface moisture content and hence through-thickness profile during the period of the test. For both reasons, it was therefore not possible to use the technique to obtain useful through-thickness profiles for the composite samples. The addition of a climate-controlled sample chamber to fit the NMR Mouse in future work could help towards this.

In order to obtain the optimal signal for sample comparison, a slice central to each sample was selected. The fully conditioned samples were expected to have a uniform moisture content over one slice thickness in the middle, and this would not be expected to change much in the time of one measurement. The position was identified by a “rough and ready” profile, using only 30 echoes and 100 scans per point. The amplitude of the first few echoes for each point was sufficient to identify the increased response corresponding to the presence of the sample. With the slice then centered on the maximum response, a full T_2 relaxation measurement was taken.

3.3 Fitting of Raw Data

Typical sets of averaged points for a single measurement are shown in Fig. 3a, with lighter dots for resin and darker dots for composite, expanded in Fig. 3b. The raw data represent the amplitude of each echo, in the instrument units of millivolts. In order to

Table 2 Main CPMG parameters

Parameter	Units	Value	Description
Spacer Δ	mm	4	Physical spacers change the distance between the RF coil and the excited sensitive volume of the sample. The smaller this is, achieved by increasing the spacer thickness, then the better the signal. But this also limits the thickness of sample that can be measured
Pulse length t_p	µsec	2.59	Duration of the CPMG pulses
Number of echoes N_e	–	8148	Number of echo pulses and corresponding amplitude values per scan
Echo time t_e	µsec	27	Time between echoes
Dwell time t_d	µsec	0.5	Delay between measurement points
Number of points N_p	–	8	Number of measurement points per echo. Dwell time × number of points = acquisition time (=4 µsec)
Repetition time t_R	ms	1000	Time between repeated CPMG sequences (scans). This needs to be long enough to allow sufficient recovery of magnetisation
Number of scans N_s	–	1000	Number of repeated CPMG sequences, averaged for final result

carry out comparisons between samples, these needed to be parameterised in some way. Typically T_2 relaxation traces can be represented by an exponential curve, but a single exponential did not match the data well. It was found that a better match to the resin curves could be obtained using a bi-exponential curve as in Eq. 1.

$$A(t) = A_1 \exp(-t/t_1) + A_2 \exp(-t/t_2) \tag{1}$$

This combines two curves, with timescales t_1 and t_2 and amplitudes A_1 and A_2. The dotted curve in Fig. 3a, b shows the bi-exponential fitting to the measured points for the resin.

It was clear that the resin and composite showed very different behaviour. The resin signal decayed to zero within around 5 ms, whereas the composite signal was still non-zero in some cases after 220 ms. The bi-exponential behaviour of the resin would be expected to still be present in the composite, so the longer term decay would need at least one extra term. In fact a single extra term was not sufficient and fitting using at least a quad-exponential curve was needed as shown in Eq. 2, i.e. two terms were required to represent the additional composite behaviour. The solid curve in Figs. 3a, b shows the quad-exponential fitting to the measured points for the composite.

$$A(t) = A_1 \exp(-t/t_1) + A_2 \exp(-t/t_2) + A_3 \exp(-t/t_3) + A_4 \exp(-t/t_4) \tag{2}$$

It should be noted that in each case the number of terms used was a balance between the visual quality of the match, the residual error achieved, and the stability of the fitting process. Distinguishing of multi-component exponentials at an appropriate noise level can be problematic [16], the data was inherently noisy, and the use of too many terms resulted in an increase in variability of the parameters for little reduction in error. In addition, the actual relaxation times potentially had a continuous distribution, which would lead to the amplitude signal given by Eq. 3.

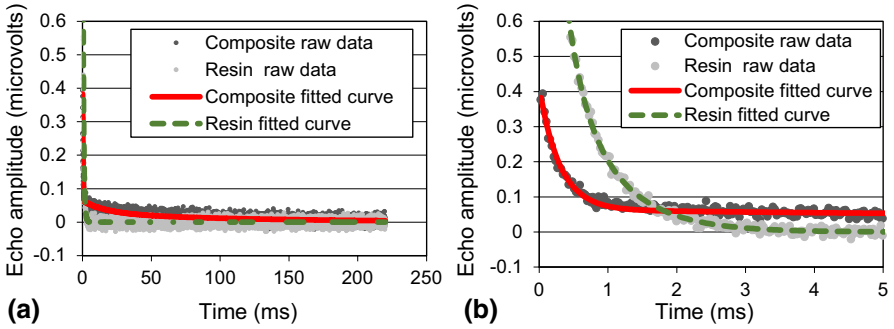

Fig. 3 Example of NMR Mouse raw data and fitted curves for resin and composite. **a** Full time period. **b** First 5 ms

$$A(t) = \int f(1/T)\exp(-t/T)d(1/T) \tag{3}$$

The likely distribution of relaxation times was checked using a Laplace transform method. For the resin alone, two peaks were obtained at times which closely matched the bi-exponential fitting. The results for the composite were more affected by the exact transform settings but showed peaks clustering around the times obtained from the quad-exponential fit. This suggested that the distribution of relaxation times was concentrated in particular ranges which corresponded to physical behaviour. Despite these uncertainties, the fitted curves led to sensible results. They also improved the clarity of comparative plots, and all the following plots use the fitted curves. Timescales were referenced in increasing order, i.e. t_1 was the shortest and t_4 the longest.

3.4 Effect of Conductivity

When comparing the fitted curves for composite samples, it was found that samples which should have been similar showed significant differences, as shown in Fig. 4a for six separate samples which had all reached a steady weight at 50 °C/85% RH. Repeated tests carried out on a single sample were consistent, indicating that this was not a result of instrument variability. It was concluded that differences in the exact sample microstructure, and hence conductivity, caused differences in eddy currents, so that the resulting signal varied from sample to sample. This was a similar effect to that observed by Brady et al. [15] when fibre damage occurred. The range of variation was comparable to about 70% of the difference between tracked samples at 50 °C/45% RH and 50 °C/85% RH, so was not insignificant.

3.5 Compensation Method

As part of the tuning of the NMR Mouse system, a check is made on the resonant frequency of the instrument. The reflected signal amplitude is measured as the transmitter frequency is varied, and at the resonant frequency this reaches a minimum. The resonant frequency of the NMR Mouse is 18.77 MHz, and a better signal is obtained the closer the actual transmitter frequency is to this.

A test was carried out using a 6 mm thick block of the same composite material as the samples, and the magnet and probe were moved upwards (cf. Fig. 1). As the composite approached the RF coil, the minimum of the curve became less pronounced, and the resonance frequency moved to higher frequency. This was in line with results found by Lind et al. [13]. For the 1 mm composite samples, although this effect was less pronounced, it was still present. Figure 5 compares the reflected signal amplitude plots obtained for a resin and a composite sample. Whilst the resin showed a sharp peak with a minimum at around 10 microvolts, the composite peak was broader, and the minimum value was much greater. The composite showed significant variation in the tuning curves from sample to sample. The "best" samples, i.e. those with least interference from eddy currents, had a minimum at around 40 microvolts.

Rather than simply accepting this sample variability and potentially dealing with it by averaging repeat samples, an attempt was made to compensate for the effect of eddy currents in some way. In order to do this, it was necessary to derive a parameter from the reflected signal curve which would represent the size of the eddy current effect. Possible values included the amplitude at the minimum, the area of the peak, or the "height" of the peak. This value would then need to be related in some, condition independent, way to the "quality" of the CPMG signal. The indicator for the latter was taken as the total area under the fitted CPMG curve. For the quad-exponential curve in Eq. 2, this is calculated as in Eq. 4.

$$Curve\ area = A_1 t_1 + A_2 t_2 + A_3 t_3 + A_4 t_4 \tag{4}$$

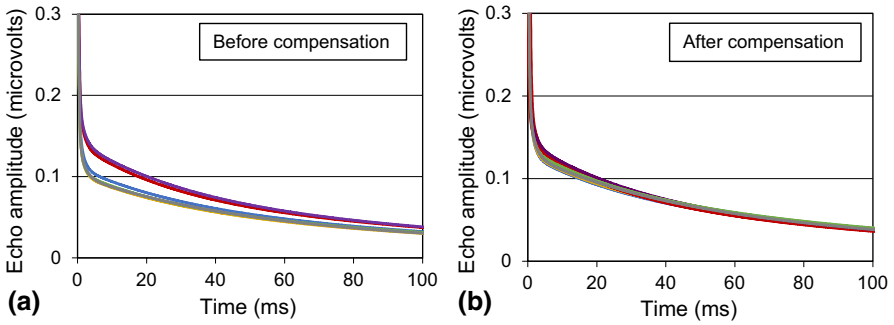

Fig. 4 CPMG curves for six composite samples conditioned to steady state at 50 °C/85% RH. **a** Before compensation. **b** After compensation

The curve area would naturally vary with sample water content, so the dependency on the eddy current effect could only be derived from samples expected to be at the same condition. To do this, tests were done on repeat samples saturated to the same condition. Curve areas for these were plotted against the various candidates for the eddy current parameter, and it was found that the reflected signal amplitude at the minimum (rather than the peak area or height) was the most useful measure.

For each condition, a line was fitted to the plot of curve area against reflected signal minimum, giving Eq. 5.

$$\widehat{Curve\ area} = \alpha\varphi + \beta \tag{5}$$

where $\widehat{Curve\ area}$ is the linear estimate of the area under the CPMG curve, φ is the reflected signal minimum, α is the slope and β the intercept. Since the CPMG signal decreased as the reflected signal minimum increased, α was negative. Figure 6a gives an example of this for samples conditioned at 50 °C/85% RH.

The area under the CPMG curve would be expected to vary with water content and hence conditioning humidity (as is demonstrated in Sect. 4), so the intercept (i.e. the "best" signals) on these plots varied as the relative humidity changed. However, it was found that the slope also varied with humidity, and that the slope was approximately a fixed multiple of the intercept, as shown in Fig. 6b.

An estimate $\hat{\alpha}$ of the slope could therefore be obtained as in Eq. 6,

$$\hat{\alpha} = k\beta \tag{6}$$

which leads to the approximate expression in Eq. 7.

$$\widehat{Curve\ area} = \beta\,(1 + k\varphi) \tag{7}$$

Here, β is condition-dependent, but k has a single value fitted over all conditions.

This enabled the CPMG curves to be normalised to a specified value of the reflected signal minimum φ to reduce any effect from variation in conductivity. The value of φ used was 40, roughly corresponding to the best value obtained during the tests. A scaling factor μ was calculated as in Eq. 8,

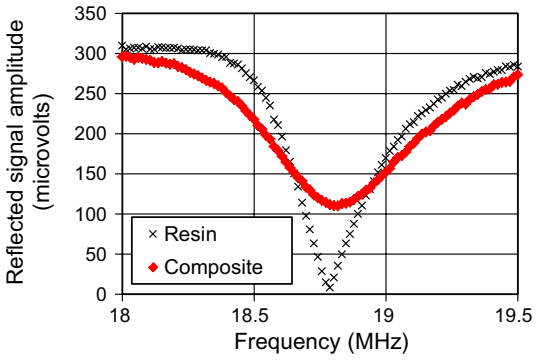

Fig. 5 Typical reflected signal amplitude curves for a resin and a composite sample

$$\mu = \left(\widehat{Curve\ area}\ \ (\varphi = 40)\right) / \left(\widehat{Curve\ area}\ \ (\text{actual}\ \varphi)\right) = (1 + 40k)/(1 + \varphi k) \tag{8}$$

and then each of the four fitted amplitudes was scaled by this value, i.e. as given by Eq. 9.

$$Adjusted\ amplitude = \mu \times Measured\ amplitude \tag{9}$$

It would have been possible to generate more detailed dependencies for the above graphs, for example using polynomial equations, or a straight line not constrained to go through the origin. However, this would have led to condition-dependent variables remaining in the final multiplying factor, when the intention was to have a factor purely dependent on the resonant frequency check.

After applying the scaling factor, the results for samples from the same condition were much more consistent, as shown in Fig. 4b which plots the same curves as in Fig. 4a but after compensation. This method was therefore applied to all the composite sample results.

4 Results and Discussion

4.1 Comparison of Resin and Composite

As detailed in Sect. 3.3, a bi-exponential function was found to give an optimal match to the resin decay curves. The existence of two decay timescales indicated protons at two levels of "boundness". A simple explanation would have been that the shorter timescale corresponded to protons in polymer molecules, whilst the longer timescale represented those in water. However the presence of water increased the amplitude of the signal at both timescales by a similar amount. This indicated water in nominally two states, probably depending on its location

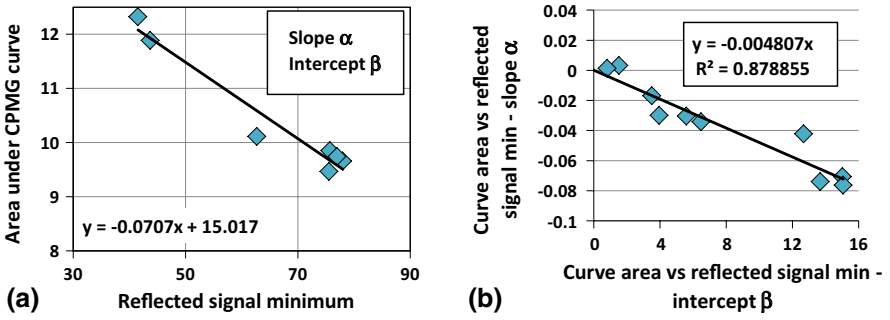

Fig. 6 Fitting of data to obtain compensation factor. **a** Plot of CPMG curve area against reflected signal minimum for samples conditioned to steady state at 50 °C/85% RH, showing fitted estimate i.e. Eq. 5 (black line). **b** Plot of slope α vs intercept β obtained from Eq. 5 for all conditions, showing fitted estimate i.e. Equation 6 (black line)

within the molecular structure of the polymer. The number of fitting parameters was limited by the rapid decay of the signal and the noise level, so as discussed above the two curves may have approximated a spectrum of behaviour representing a range of states of water, but concentated around two relaxations representing physical effects.

For the composite, although the signal period was longer, the noise level was considerably greater. Despite this, the signals were good enough to show that an additional two exponential functions were needed, but these were found to be the maximum that the data could robustly support. As for the resin, these may have represented a spectrum of actual "boundness" of the water. Figure 7 gives an example of the separate components of the amplitude curve. Figure 7a shows the rapid decay in the resin corresponding to t_1 and t_2, whilst Fig. 7b shows the longer-term effects in the fibres, where t_3 and t_4 dominate.

The difference between resin and composite suggested that the longer timescale came from the fibres. A sample of the carbon fibres alone was tested, although the results were somewhat approximate as water movement in or out of the fibres was very fast so the conditions changed during the test. Figure 8a shows the resulting curve for the fibres, compared with those for resin and composite. The fibre signal required a bi-exponential curve with timescales (shown in Table 3) much higher than those of the resin and closer to the t_3 and t_4 values for the composite, confirming that the longer timescales resulted from the presence of the fibres.

4.2 Condition Dependency

Relaxation curves for samples from various temperatures and humidities are plotted in Fig. 8b for resin and Fig. 8c for composite. Table 3 shows the corresponding fitting parameters for resin, and for the fibre sample shown in Fig. 8a. Since the number of composite samples was considerably larger, their amplitude and time constant values are shown graphically in Sect. 4.3.

For the resin, the two rapid relaxations occurred for samples over the whole range of humidities. The timescale and amplitude of both relaxations increased with increasing water content. The signal from the dry sample was thought to come from the hydrogen nuclei of the polymer molecules. As water was absorbed, initially (i.e. at 45% RH) the two timescales changed little, with just an increase in amplitude for both relaxations. At 85% RH, the longer time constant increased significantly as did the corresponding amplitude, suggesting more absorption into slightly less bound sites. The amplitude for the short relaxation actually went down slightly for the 85% RH sample, suggesting that there was saturation of the most bound water by this point.

In Fig. 8c, the initial part of the composite curves for a range of humidities is shown. Again, there was a clear increase in amplitude with water content. The curves for dry material did not drop to zero as quickly as those for resin, which suggested that either some residual water was present, or that there was a signal from other molecules with greater freedom associated with the fibres, possibly attached functional groups.

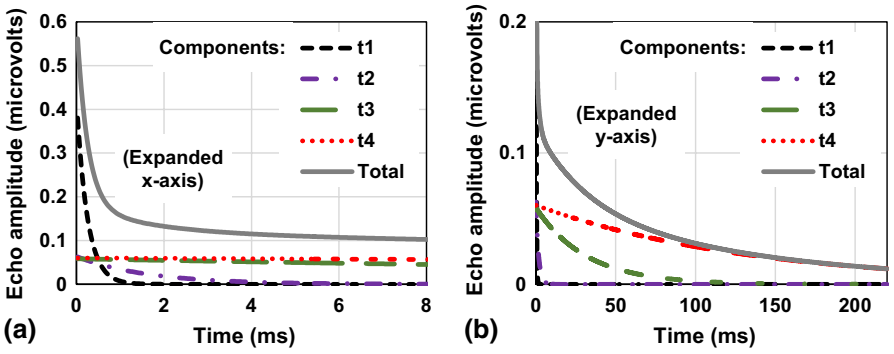

Fig. 7 Example of decomposition of quad-exponential curve into its component parts. **a** First 8 ms, full amplitude axis. **b** Full time period, expanded amplitude axis

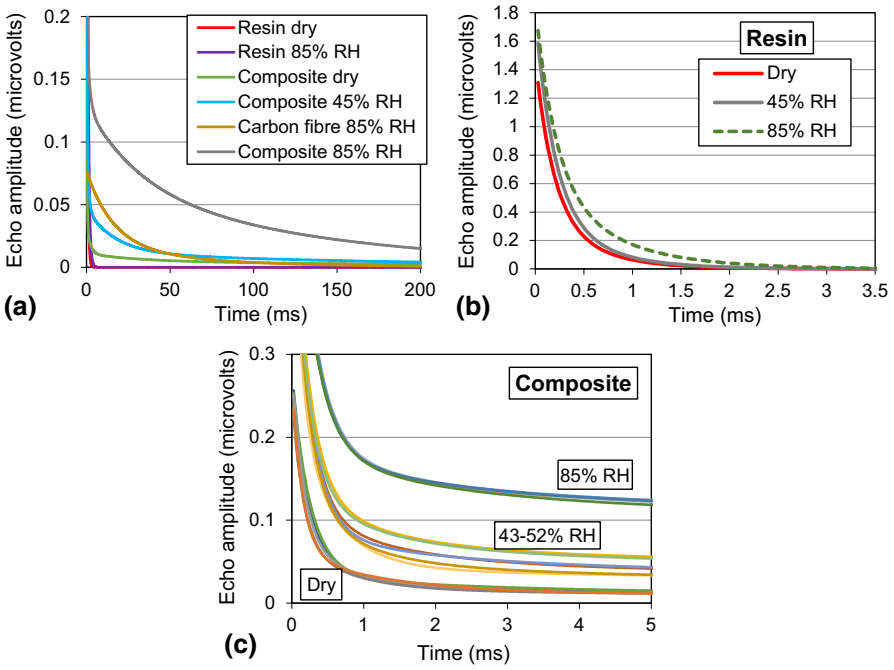

Fig. 8 CPMG curves. **a** Carbon fibre compared to resin and composite (legend order corresponds to curves from low to high amplitude). **b** Resin samples at various humidities. **c** Composite samples at various humidities (expanded time axis)

4.3 Time Constant and Amplitude Graphs for Composite Samples

4.3.1 Resin-Related Timescales

Figure 9 shows the time constants and amplitudes for the two faster relaxations in all the composite samples, plotted against total water content. The shortest time

Table 3 Fitting parameters for CPMG curves for resin and carbon fibres

Material	Condition	Time constants (ms)				Amplitudes (microvolts)			
		1	2	3	4	1	2	3	4
Resin	70 °C-dry	0.19	0.54			1.10	0.38		
Resin	70 °C-45% RH	0.20	0.56			1.34	0.43		
Resin	70 °C-85% RH	0.21	0.73			1.21	0.64		
Fibres	70 °C 85% RH			15.9	65.9			0.059	0.017

constant, t_1, was comparable to that of the resin, and increased only a little as the water content increased, whilst the amplitude increased rapidly with water content up to about 3% but then levelled off. This suggested a signal from the polymer protons in dry material, which was increased during initial water absorption by water molecules strongly linked to the polymer chain so that their proton relaxation time was only slightly longer than that of the polymer protons. These would correspond to the "bound" water of Carter and Kibler [12]. The longer of the two resin timescales, t_2, whilst being clearly defined for each individual sample, was more variable. Both the time constant and amplitude at this scale increased slightly with water content. This suggested absorption of more mobile water [12], with the resulting polymer swelling also increasing the relaxation time.

4.3.2 Fibre-Related Timescales

Figure 10 shows the time constants and amplitudes for the two slower relaxations in all the composite samples, plotted against total water content. The time constant t_3 increased gradually with increasing water content, whilst the corresponding amplitude increased significantly from dry to around 6% water content then levelled off. The initial value for t_3 was similar to the lower time constant measured for the carbon fibres. The levelling off indicated a separate phase, which eventually filled up or became less attractive. This would correspond to the adsorption of water molecules on to the surface of the fibres as suggested by Do and Do [3].

As the water content increased from dry to around 4%, the amplitude corresponding to t_4 only increased slightly. At water levels below about 4% the value of t_4 was apparently higher but was also very noisy due to the difficulty of fitting time constants to signals of very low amplitude, and so interpretation of this should be cautious. The water giving the t_4 relaxation would correspond to molecule clusters within the fibre pores, where they had a high degree of freedom compared to those adsorbed on to the surface. If there were voids between fibres and resin as a result of incomplete surface wetting, these would show similar behaviour. Initially there would be few molecule clusters, but above about 4% water content the long-term amplitude increased significantly, roughly corresponding to the point at which the t_3 amplitude levelled off, and water on the fibre surfaces was moving in much larger quantities into freer clusters within the pores. The time constant continued to fall slightly in this region as the number of clusters in the pores increased leading to

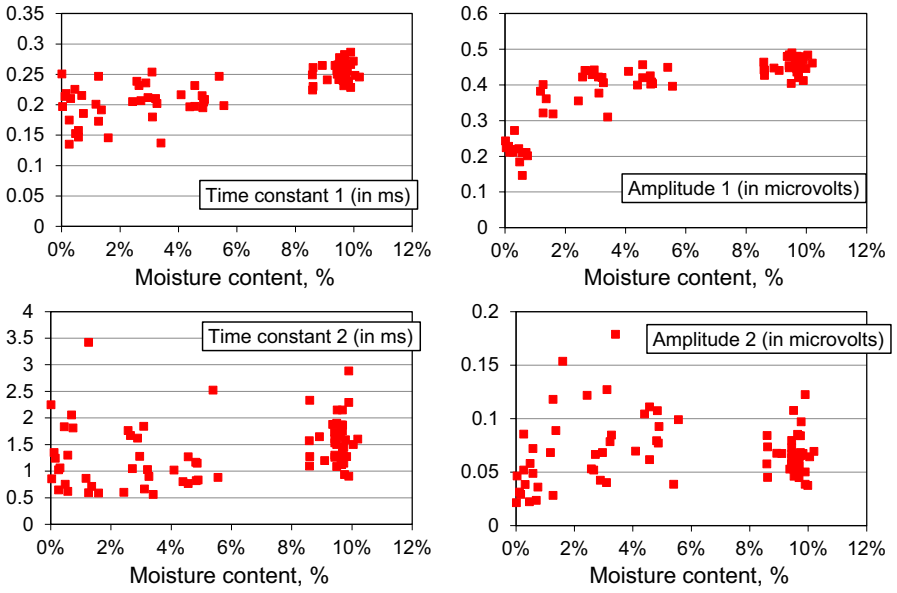

Fig. 9 Time constants and amplitudes for resin-related relaxation, as a function of water content

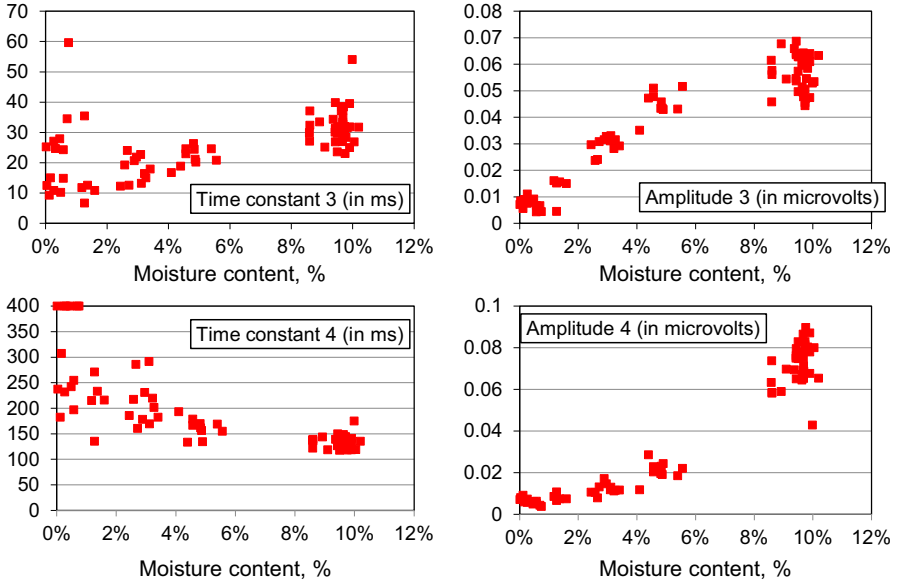

Fig. 10 Time constants and amplitudes for fibre-related relaxation, as a function of water content

greater interaction. t_4 was also higher than the relaxation time seen for the fibres alone. If the water giving this relaxation (~150 ms) was assumed to be the water in the fibre pores, then it still had a much faster T_2 relaxation than free water (~2 s) but had a slower relaxation than the least bound water in the fibres alone (~66 ms). This showed that the water in the fibre pores was still partly bound by the fibre surfaces, and with the fibres alone, rapid loss of water from exposed fibres during testing increased the proportion bound to the surfaces.

5 Conclusion

The water absorption in carbon fibre/phenolic samples was successfully studied using single-sided NMR despite the problems incurred as a result of the electrical conductivity of the fibres. Samples were cut at an angle to the lay-up plane to reduce conductivity effects, and a method was found to compensate for the sample-to-sample variation resulting from differences in microstructure. Measurement of T_2 relaxation was enabled which gave an insight into the form in which water was held within the material.

The observed behaviour for the composite could be correlated with that proposed for activated carbon fibres [3]. Water moving into the material was initially most attracted to tightly bound sites in the resin, though some water was in less tightly bound resin sites. This behaviour was seen in the samples of resin alone. With the composite, additional water was present in less constrained sites, thought to be adsorbed on to fibre surfaces, and this saturated when the moisture content reached around 6%. Above about 4% moisture content, water was identified which was less bound again, attributed to water gathered in clusters within the fibre pores. Both of these types of water were seen on the carbon fibres when tested alone.

Overall, the NMR Mouse has proved to be a very useful technique for characterising the nature of water absorbed into composites, even in complex materials such as the carbon fibre/phenolic systems tested here. There are several experimental challenges to overcome with testing different materials, in particular the need for methods to address the problem of sample conductivity.

References

1. J. Feldman, D. Ellerby, M. Stackpoole, K. Peterson, E. Venkatapathy, 3D Woven Thermal Protection Systems. (NASA website), https://ntrs.nasa.gov/archive/nasa/casi.ntrs.nasa.gov/20150022378.pdf. Accessed May 2020.
2. E.H. Stokes, AIAA J. **30**(6), 1597–1601 (1992)
3. D.D. Do, H.D. Do, Carbon **38**, 767–773 (2000)
4. Magritek, NMR-Mouse one-sided NMR. (Magritek website), https://www.magritek.com/products/nmr-mouse. Accessed 21 May 2020.
5. B. Blümich, J. Perlo, F. Casanova, Progr. Nucl. Magn. Reson. Spectrosc. **52**(4), 197–269 (2008)
6. B. Blümich, S. Haber-Pohlmeier, W. Zia, *Compact NMR* (Walter de Gruyter GmbH, Berlin/Boston, 2014). **(ISBN 978-3-11-026628-3 e-ISBN 978-3-11- 026671-9)**
7. F. Casanova, J. Perlo, B. Blümich (eds.), *Single-Sided NMR* (Springer, Berlin, Heidelberg, 2011). **(ISBN 978-3-642-16306-7 e-ISBN 978-3-642-16307-4)**
8. A. Guthausen, G. Zimmer, P. Blümler, B. Blümich, J. Magn. Reson. **130**, 1–7 (1998)
9. K.-P. Hoh, H. Ishida, J.L. Koenig, Polym. Compos. **11**(3), 192–199 (1990)
10. J. Kolz, in: *Single-Sided NMR*, ed. by F. Casanova, J. Perlo, B. Blümich (Springer, Berlin, Heidelberg, 2011) pp 216–217. ISBN 978–3–642–16306–7 e-ISBN 978–3–642–16307–4
11. S. Popineau, C. Rondeau-Mouro, C. Sulpice-Gaillet, M.E.R. Shanahan, Polymer **46**, 10733–10740 (2005)
12. H.G. Carter, K.G. Kibler, J. Compos. Mater. **12**(2), 118–131 (1978)
13. A.C. Lind, C.G. Fry, C.H. Sotak, J. Appl. Phys. **68**, 3518–3528 (1990)
14. V.M. Bouznik, E.V. Morozov, I.A. Avilova, V.I. Volkov, Appl. Magn. Reson. **47**, 321–334 (2016)
15. S.K. Brady, M.S. Conradi, C.M. Vaccaro, J. Magn. Reson. **172**, 342–345 (2005)
16. C. Lanczos, *Applied Analysis* (Dover Publications Inc, New York, 1988), pp. 272–280. **(ISBN 0-486-65656-X)**